



**Electrofacies Characterization in Lacustrine Coquinas and Hybrid Deposits from Rift Phase: Pre-Salt, lower Cretaceous, Campos Basin, Brazil**

Caracterização de Eletrofácies em Coquinas Lacustres e Depósitos Híbridos de Fase Rifte: Pré-Sal, Cretáceo inferior, Bacia de Campos, Brasil

Vinicius Carbone Bernardes de Oliveira<sup>1,2</sup>; Felipe Vasconcelos dos Passos<sup>1,2</sup>;  
Carlos Manuel de Assis Silva<sup>1</sup> & Leonardo Borghi<sup>2</sup>

<sup>1</sup>Centro de Pesquisa e Desenvolvimento da Petrobras,

Avenida Horácio de Macedo 950, 21949-915, Ilha do Fundão, Cidade Universitária, Rio de Janeiro, RJ, Brasil

<sup>2</sup>Universidade Federal do Rio de Janeiro, Programa de Pós-Graduação em Geologia,

Centro de Ciências Matemáticas e da Natureza, Instituto de Geociências, Departamento de Geologia, Avenida Athos da Silveira

Ramos 274, Bloco F, 21949-900, Ilha do Fundão, Cidade Universitária, Rio de Janeiro, RJ, Brasil

Emails: [viniciuscarbone@petrobras.com.br](mailto:viniciuscarbone@petrobras.com.br); [felipevp@petrobras.com.br](mailto:felipevp@petrobras.com.br); [carlosmas@petrobras.com.br](mailto:carlosmas@petrobras.com.br); [lborghi@geologia.ufrj.br](mailto:lborghi@geologia.ufrj.br)

Recebido em: 10/04/2019      Aprovado em: 20/05/2019

DOI: [http://dx.doi.org/10.11137/2019\\_3\\_178\\_191](http://dx.doi.org/10.11137/2019_3_178_191)

## Resumo

Esse estudo apresenta modelos de eletrofácies para dois poços com testemunhos e amostras laterais da Formação Coqueiros, Cretáceo inferior da Bacia de Campos. O POÇO-1 está localizado em águas profundas no sul da bacia e é composto por rochas carbonáticas bioclásticas, siliciclásticas e rochas híbridas. A modelagem de eletrofácies para esse poço distinguiu quatro eletrofácies que são correlacionadas às litofácies de coquina, rocha híbrida, lamito e arenito. O POÇO-2 está situado em águas ultra profundas no norte da bacia e é essencialmente composto por carbonatos bioclásticos. Para esse poço, a modelagem de eletrofácies diferenciou quatro eletrofácies, que são correlacionadas às litofácies de lamito, coquina com lama carbonática, coquina com conchas fragmentadas e/ou orientadas, e coquinas maciças, mal selecionadas com grau variável de fragmentação das conchas. Este estudo mostrou que é possível distinguir, com elevado grau de precisão, rochas carbonáticas bioclásticas de rochas siliciclásticas e híbridas baseando-se em perfis de poço. A análise de eletrofácies distinguiu rochas carbonáticas suportadas por partículas daquelas suportadas por lama. Também foi possível separar rochas carbonáticas bioclásticas com diferentes critérios tafonômicos, como organização e grau de fragmentação das conchas. O modelo de eletrofácies demonstrou-se uma ferramenta útil para interpretar intervalos geológicos sem amostras de rocha. No entanto, modelos de eletrofácies nunca irão representar todas as várias fácies deposicionais, e assim não podem substituir totalmente a amostragem de rocha em estudos sedimentológicos e de reservatório de detalhe.

**Palavras-chave:** fácies perfil; coquinas; rochas híbridas

## Abstract

This study presents electrofacies models for two wells with cores and sidewall cores of Coqueiros Formation, lower Cretaceous of Campos Basin. The WELL-1 is located in deep water of the south of the basin and is composed by bioclastic carbonate, siliciclastic and hybrid rocks. The electrofacies modelling distinguished four electrofacies, which are correlated to the lithofacies coquina, hybrid rock, siliciclastic mudstone, and sandstone. The WELL-2 is situated in ultra-deep water of the north of the basin and is essentially constituted of bioclastic carbonates. The electrofacies modelling for this well differentiated four electrofacies, which are correlated to the lithofacies mudstone, coquina with carbonate mud, coquina with moderate to high degree of shell fragmentation and/or oriented shells, and poorly sorted massive coquina with variable degree of shell fragmentation. This study showed that it is possible to distinguish, with high level of accuracy, bioclastic carbonate rocks from siliciclastic and hybrid rocks based on the well logs. The electrofacies analysis distinguished particle-supported carbonate rocks from mud-supported ones. It was also possible to separate bioclastic carbonate rock with different taphonomic criteria, such as organization and degree of shell fragmentation. The electrofacies model showed to be a useful tool to interpret geological intervals in wells without rock samples. Nevertheless, it will never represent all the numerous depositional facies, and thus it can not completely replace the rock sampling in detailed sedimentological and reservoir studies.

**Keywords:** lofacies; coquinas; hybrid rocks



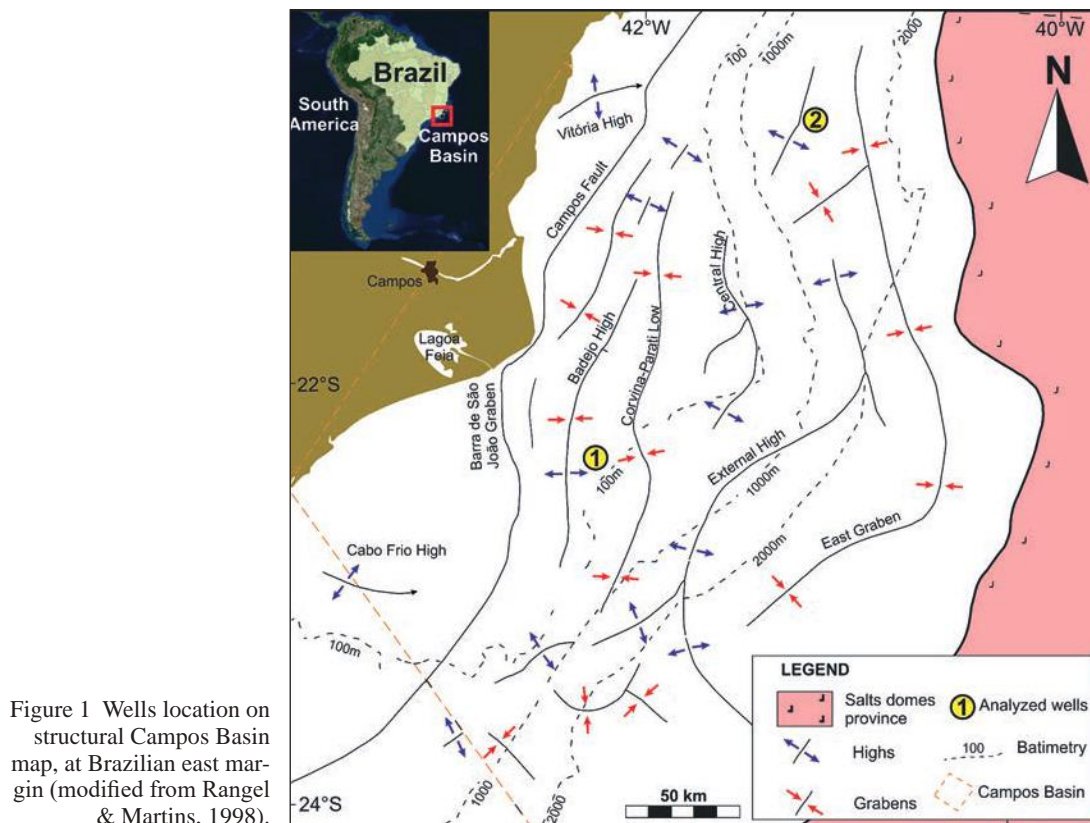
## 1 Introduction

Recent discoveries of large oil accumulations in Pre-Salt coquinas in Santos and Campos basins' deep waters demanded new studies to improve the geological characterization of these reservoirs (Mello, 2008; Petersohn & Abelha, 2013; Carlotto *et al.*, 2017; ANP, 2017a,b). Traditional studies of these reservoirs are mainly based on core data and the observation of core and thin sections are used to identify the various types of lithofacies. However, due to high costs of a Pre-Salt drilling rig (Morais, 2013), it is not always possible to obtain core samples and these reservoir rocks are often sampled by sidewall cores instead of whole cores. Therefore, in order to have a continuous information of probable lithofacies in non-cored intervals, the recourse to electrofacies modelling from well log data may be an alternative way. Electrofacies are defined as the result of a set of well log responses, which characterizes a bed that can be distinguished from the adjacent ones (Serra & Abbot, 1982).

Electrofacies analysis has been widely applied in siliciclastic successions (Johnson *et al.*, 1987; Fle-

xa *et al.*, 2004; Stinco, 2006; Tang & White, 2008; Schmitt *et al.*, 2013; Grou, 2015) because distinct lithofacies with variable composition and fabrics result in distinct log responses. Nevertheless, this method can be also applied to carbonate sequences, even though they generally have more homogeneous composition (Baumgardt & Scuta, 1989; Tang *et al.*, 2011; Rezaeeparto *et al.*, 2016; Al Ibrahim *et al.*, 2017). In Campos Basin Coqueiros Formation, the first petrofacies study was done by Horschutz & Scuta (1992). More recently, Correa (2016) used electrofacies analysis to distinguish diagenetic products in the Coqueiros Formation.

The objective of this work is to characterize the electrofacies and to measure the similarity with lithofacies of cores and sidewall cores of two wells in the Campos Basin. The results will be useful for evaluating the applicability of electrofacies for lithofacies prediction in non-cored intervals. This work shows electrofacies studies for two wells in Campos Basin. WELL-1 is located on the Badejo High, in shallow water, at the south of Campos Basin. WELL-2 is situated on the Outer High, in ultra-deep waters, at the north of Campos Basin (Figure 1).



## 2 Geological Setting

The Campos Basin, located on the Brazilian continental margin, was formed during Early Cretaceous, as a result of the Gondwana Supercontinent break-up, which occurred with intense volcanic activity (Conceição *et al.*, 1988; Dias, 2005). During the rift phase, the tectonic pattern was characterized by horsts, grabens and half-grabens, formed by synthetic and antithetic normal faults with SW-NE strike (Dias *et al.*, 1990).

The most important highs in the basin are the Badejo High and the Outer High. The former is located in shallow waters of Campos Basin with a north dip (Chang *et al.*, 1990). The latter is located in deep water and represents a structural high of the basin's basement. (Rangel & Martins, 1998; Gomes *et al.*, 2002; Bastos & Luparelli, 2015). These highs are focal points for oil migration, where are located the biggest Pre-Salt oil accumulations (Gomes *et al.*, 2002; Carminatti *et al.*, 2008; Dehler *et al.*, 2016).

The sedimentation in Campos Basin can be divided in three supersequences: rift, post-rift and drift, which were deposited on top of basalt floodings of Cabiunas Formation (Winter *et al.*, 2007). In Campos Basin, Pre-Salt reservoirs are the rift and sag carbonates of Coqueiros and Macabu formations, respectively, covered by the evaporites of Retiro Formation.

The Coqueiros Formation of Lagoa Feia Group is the focus of this work. It was formed during the Late Barremian-Early Aptian (Jiquia local stage) (Winter *et al.*, 2007). This formation is characterized by shale layers intercalated with coquinas, defined by Schäfer (1972) as accumulations of shells and/or shell fragments deposited by the action of some transport agent.

## 3 Study Data and Methods

The study data are from two wells in Campos Basin (Figure 2) which sampled the Coqueiros Formation. WELL-1 is located 80 km from the coast of Rio de Janeiro State, in water depth of approximately 100 m, on the Badejo Structural High in the south of Campos Basin. WELL-2 is located 75

km from the coast of Espírito Santo State, in water depth of approximately 1300 m, on the Outer High structure in the north of Campos Basin, (Figure 1). In WELL-1 there are eight cores, totaling 105.9 m of rock, and in WELL-2 there is a 31.5 m long core and 27 sidewall cores.

In WELL-1, Coqueiros Formation is composed by carbonate, siliciclastic and hybrid rocks, interpreted as deposited in a lacustrine ramp, proximal to the rift continent margins (Figure 3) (Oliveira *et al.*, 2019). They were deposited stratigraphically underneath the conglomerates of Itabapoana Formation below the depth of 2663,4 m. In WELL-2, Coqueiros Formation is composed by carbonate sequences, locally intercalated with siliciclastic mudstones, interpreted as deposited on an isolated carbonate platform. They were deposited underneath laminites and dolomites of Macabu Formation below the depth of 4546.0 m.

The set of logs analyzed in WELL-1 is formed by gamma ray, density, neutron and acoustic. In WELL-2 the logs analyzed are gamma ray, density, neutron, acoustic, photoelectric factor, nuclear magnetic resonance, and elementals logs (Al, Ca, Fe, Si, U, and Ti). In this study, it was used a sampling interval (SI) of 20 cm. The resistivity and spontaneous potential logs were not used in this study because both wells present the oil-water contact in the studied section and distinct fluid composition will affect negatively the lithofacies prediction. The caliper log of WELL-2 was not useful, because it does not show variations in studied interval. The geological cores and sidewall cores descriptions are in Oliveira *et al.* (2019).

The modelling was performed by the multi-resolution graph-based clustering (MRGC), a multidimensional dot-pattern recognition method based on non-parametric k-nearest neighbors (KNN) and graph data representation (Ye & Rabiller, 2000). This method was chosen because it provides unbiased rapid clustering, without prior knowledge of data structure and cluster numbers, turning it ideal for unsupervised clustering (Ye & Rabiller, 2000). MRGC automatically determines the optimal number of clusters, and the level of detail can be defined

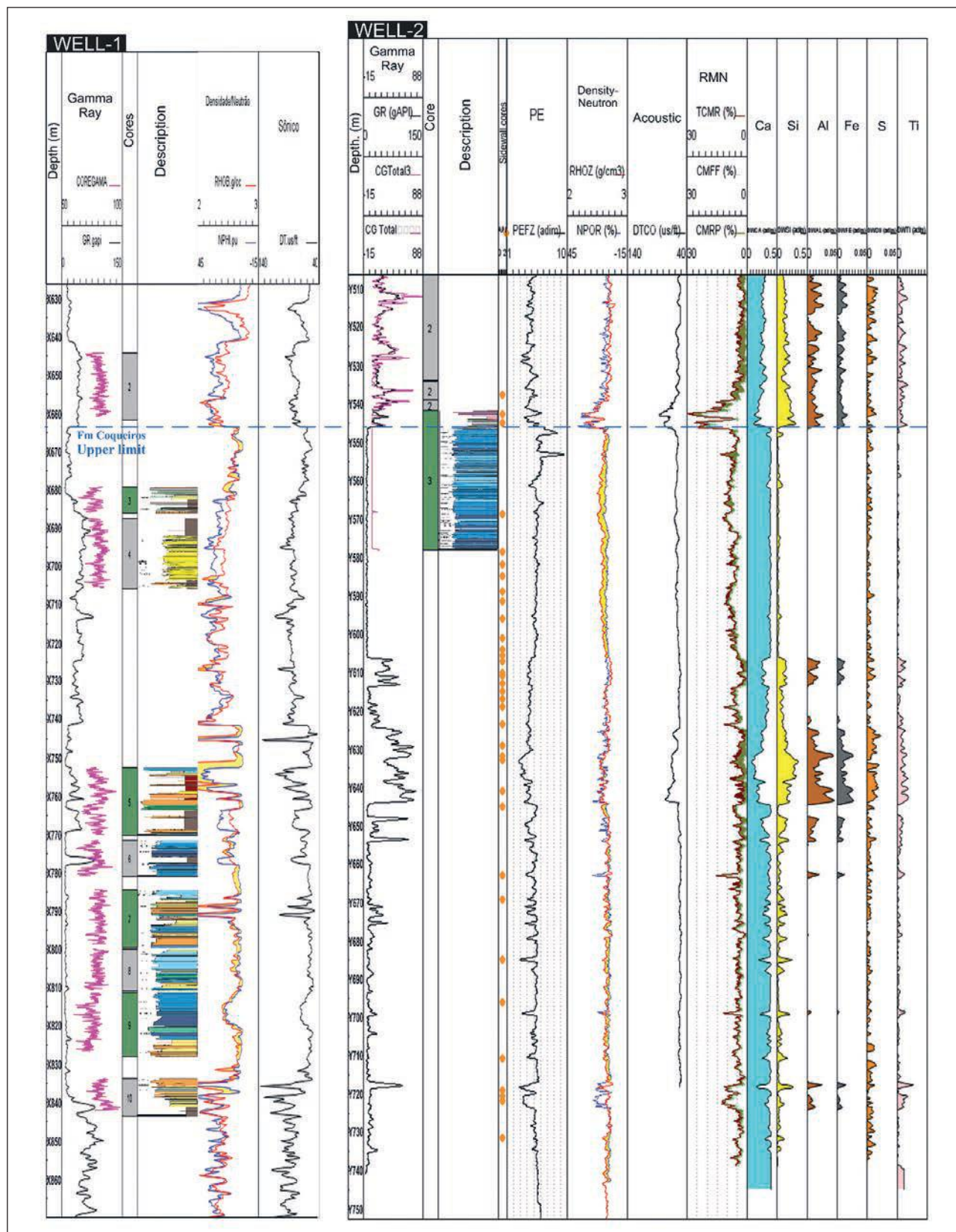


Figure 2 Study data: eight cores from WELL-1 (105.9 meters) and one core (31.5 meters) and 27 sidewall cores from WELL-2. From this samples, 183 thin sections are petrographically studied.

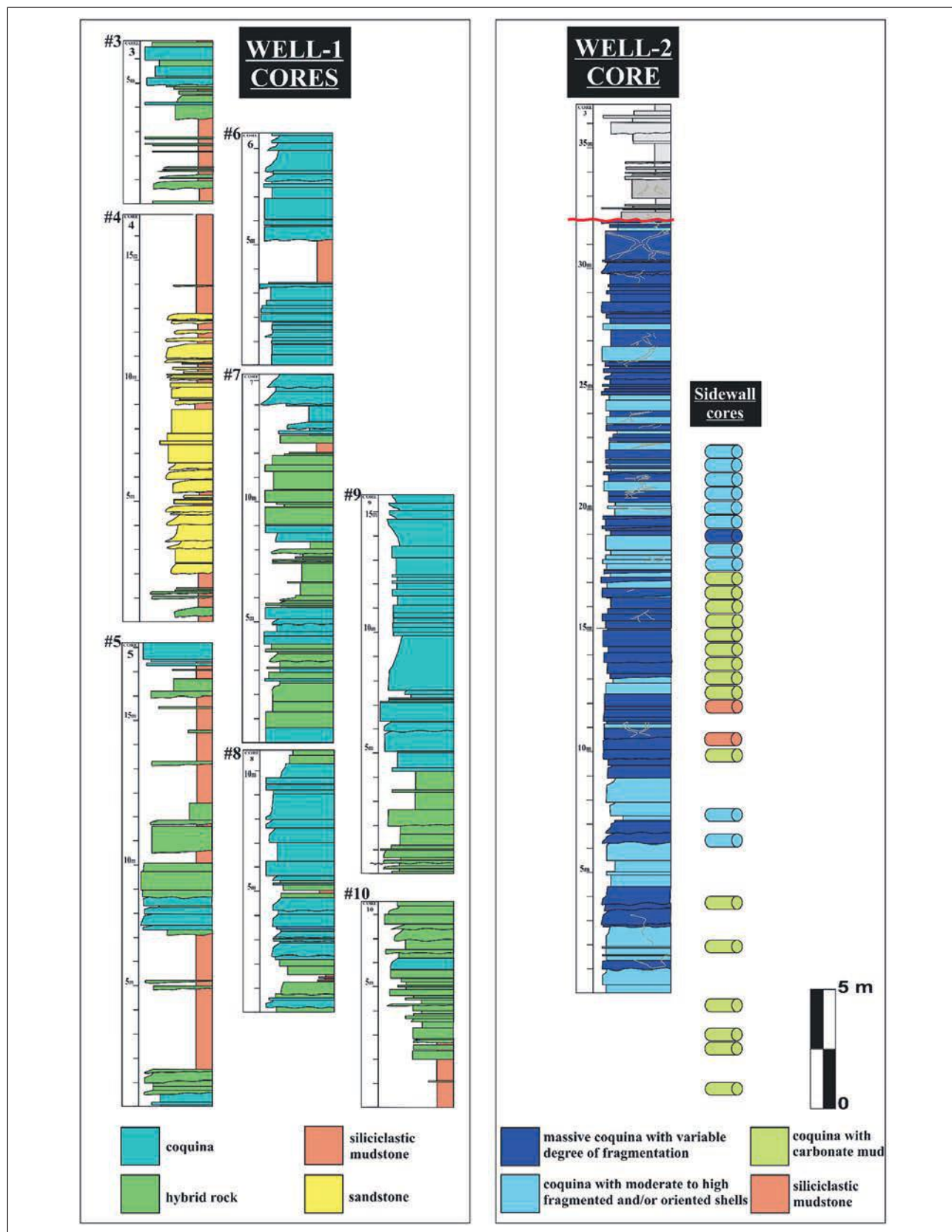


Figure 3 Cores description from WELL-1, in a hybrid geological setting, and core and sidewall cores descriptions from WELL-2, in an essentially carbonate geological setting. For samples position see Figure 2.

based on actual needs. Therefore, the model was correlated with lithofacies of cores and sidewall cores and the clusters with high accuracy in the same lithofacies were merged to form the final electrofacies. At the end, the model was propagated to all wells with K-Nearest Neighbor approach (KNN Facies Propagation) (Figure 4 Method used in this work. For WELL-1, it was used for modelling gamma ray (GR), density (DEN), neutron (NEU) and acoustic (DT). For WEEL-2 modelling, it was utilized gamma ray (GR), density (DEN), neutron (NEU), acoustic (DT), photoelectric factor (PR), nuclear magnetic resonance logs (NMR) and elementals logs (ELM).).

## 4 Results

### 4.1 WELL-1

The modelling intended to use electrofacies to individualize the main lithofacies: sandstone, siliciclastic mudstone, coquinas and hybrid rocks. The hybrid rocks are composed with less than 90% of a single component. They are constituted of a mixture of intrabasinal carbonate particles (mainly bivalve shells), extrabasinal siliciclastics grains and intrabasinal non-carbonate grains (stevensitic and volcanoclastic grains) (Oliveira *et al.*, 2019).

The MRGC method generated five models, with 5, 7, 11, 14 and 16 clusters. In order to better individualize each lithofacies, the model with 16 clusters was used, thus they were manually merged to form electrofacies of better match to lithofacies. The combinations resulted in four electrofacies (Figure 5 Synthesis of the electrofa-

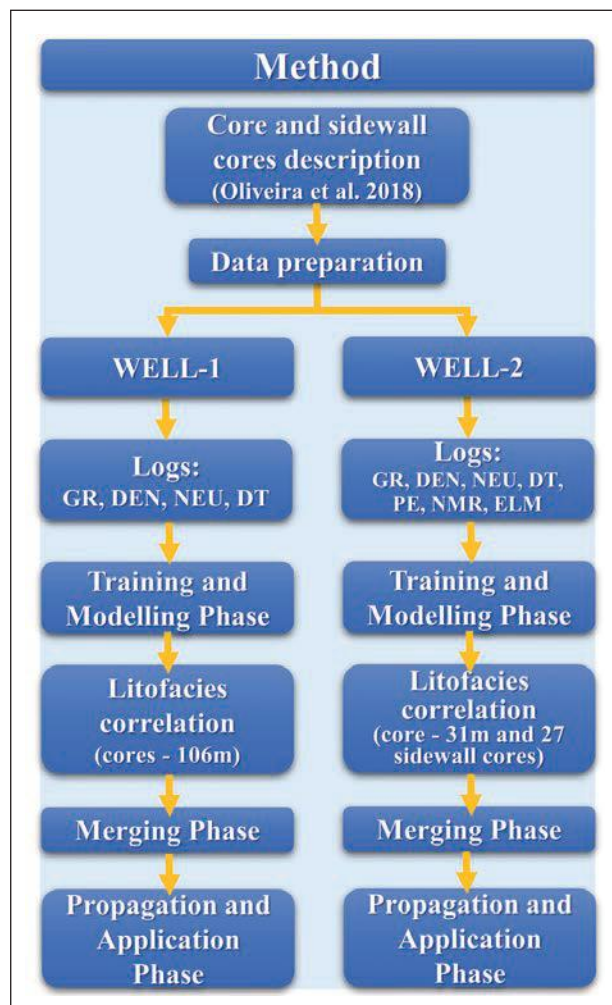
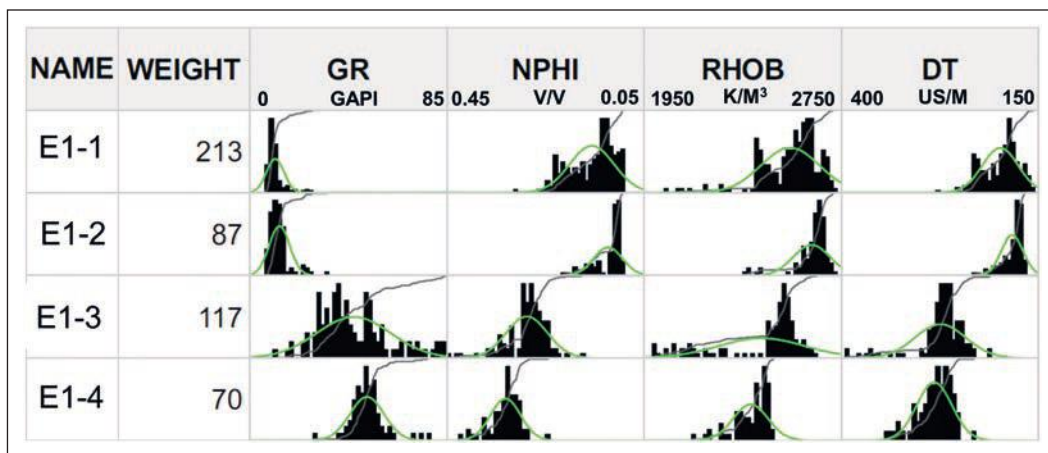


Figure 4 Method used in this work. For WELL-1, it was used for modelling gamma ray (GR), density (DEN), neutron (NEU) and acoustic (DT). For WEEL-2 modelling, it was utilized gamma ray (GR), density (DEN), neutron (NEU), acoustic (DT), photoelectric factor (PR), nuclear magnetic resonance logs (NMR) and elementals logs (ELM).

Figure 5 Synthesis of the electrofacies obtained for WELL-1, with the combination of generated clusters, and corresponding histograms for value variation from the wireline logs used in modeling.



cies obtained for WELL-1, with the combination of generated clusters, and corresponding histograms for value variation from the wireline logs used in modeling. and Figure 6). Each characterized electrofacies match a lithofacies, with different degrees of accuracy (Figure 7 Electrofacies by decreasing probability of lithofacies occurrence in WELL-1. (CQ – coquina; HB – hybrid rock; MD – mudstone; SD sandstone).).

The electrofacies E1-1 was created by combination of five clusters. The gamma ray has low values, varying from 6.7 to 12.8 API, with mean at 11.1 API. Neutron log commonly oscillates from 0.19 to 0.04 v/v, with mean equal to 0.08 v/v. Density values vary between 2399 and 2702 kg/m<sup>3</sup>, with mean at 2542 kg/m<sup>3</sup>. Sonic transit time predominantly varies between 234.6 and 162 μs/m. The correlation with core lithofacies show that this electrofacies are related to coquina (CQ) with 69% of probability.

The electrofacies E1-2 was generated by combination of three clusters. It is characterized by

gamma ray values between 7.8 and 15.3 API, with mean at 12.9 API. Neutron porosity mainly between 0.09 and 0.04 v/v. The density log has most of its values from 2565 to 2717 kg/m<sup>3</sup>, with mean equal to 2629 kg/m<sup>3</sup>. Sonic transit time oscillates mainly from 197 to 167 μs/m. This electrofacies has correlation to the lithofacies hybrid rocks (HB), with 61% of probability.

The electrofacies E1-3 was formed by combining six clusters. It is characterized by a wide range of gamma ray values, varying mainly between 28 and 58 API, with mean of 44 API. Neutron porosity results alternate roughly between 0.32 and 0.19 v/v. The density generally has values from 2449 to 2630 kg/m<sup>3</sup>. Sonic transit time oscillates mainly from 289 to 237 μs/m. This electrofacies has a good correlation with the lithofacies mudstone (MD), with 75% of probability.

The electrofacies E1-4 was generated by the combination of two clusters. The gamma ray ran-

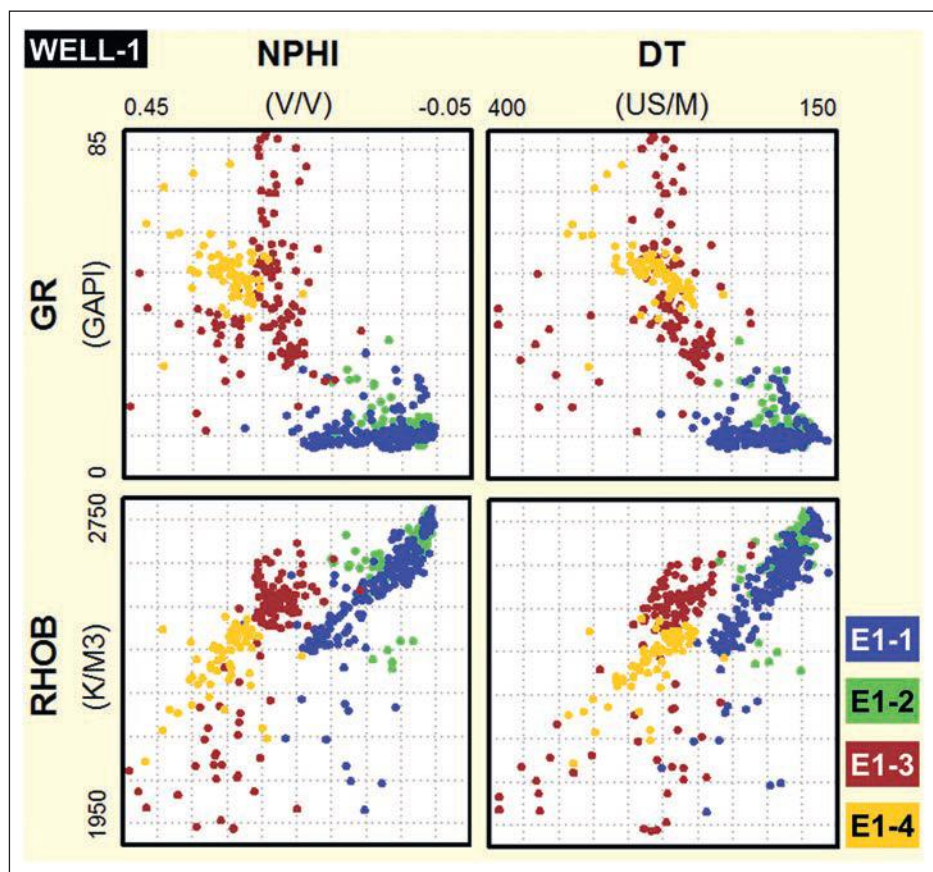


Figure 6 Electrofacies in wireline log crossplot for WELL -1.

	E1-1	E1-2	E1-3	E1-4
MOST	CQ (69%)	HB (61%)	MD (75%)	SD (69%)
	HB (28%)	CQ (33%)	HB (16%)	MD (19%)
	MD (4%)	MD (6%)	CQ (4%)	HB (13%)
LEAST			SD (4%)	

Figure 7 Electrofacies by decreasing probability of lithofacies occurrence in WELL-1. (CQ – coquina; HB – hybrid rock; MD – mudstone; SD sandstone).

ges from 43.2 to 55.3 API, with mean of 50.59 API. Neutron log has values ranging from 0.36 to 0.27 v/v. The density ranges from 2317 to 2462 kg/m<sup>3</sup>. Acoustic transit times range from 309.6 to 252.8 μs/m. This electrofacies are related to the sandstone lithofacies (SD), with 69% of probability.

#### 4.2 WELL-2

The modelling used electrofacies to individualize the main lithofacies in this well. The challenge was the distinction of carbonate rocks with very similar composition, coquinas (rudstones and grainstones of bivalves) and carbonatic mud. The carbonatic lithofacies were poorly sorted massive coquina with variable degree of fragmentation (CQm); coquina with moderate to high degree of shell fragmentation and/or oriented shells (CQf), coquina with carbonate

mud (CQu), which includes mudstones, wackestones, packstones and floatstones.

The MRGC method generates five models with options of 4, 9, 11, 15 and 19 clusters. The model with 19 clusters was chosen, so the clusters were merged based on their similarities and matched to lithofacies. The resulting model has four electrofacies (Figure 8 Synthesis of the electrofacies obtained for WELL-2, with the combination of generated clusters, and corresponding histograms for value variation from the wireline logs, with the best distinctions of values. and Figure 9), each electrofacies is correlated to lithofacies with different degrees of accuracy (Figure 10).

The electrofacies E2-1 is characterized by high gamma ray values, ranging from 92 to 130 API. Neutron porosity results ranges from 0,15 to 0,09 v/v. The density has values ranging from 2.51 to 2.64 g/cm<sup>3</sup>. Acoustic transit times range mainly from 247 to 215 μs/m. The total combinable magnetic resonance (TCMR) porosity ranges from 2.2 to 7.18%, with mean value of 4.56%. The photoelectric effect (PE) ranges from 3.3 to 4.33 b/e, with mean value of 3.81b/e. This electrofacies shows low values of calcium, measured by the dry weight of Calcium log (DWCa), that ranges from 0.12 to 0.18 w/w, and have relatively high values of silicon (DWSi), with mean value of 0,22 w/w. It presents aluminum (DWA1), ranging from to 0.028 and 0.044w/w and iron (Fe) ranging from 0.02 to 0.03 w/w. This electrofacies corresponds to the siliciclastic mudstone (MD) with probability of 100%.

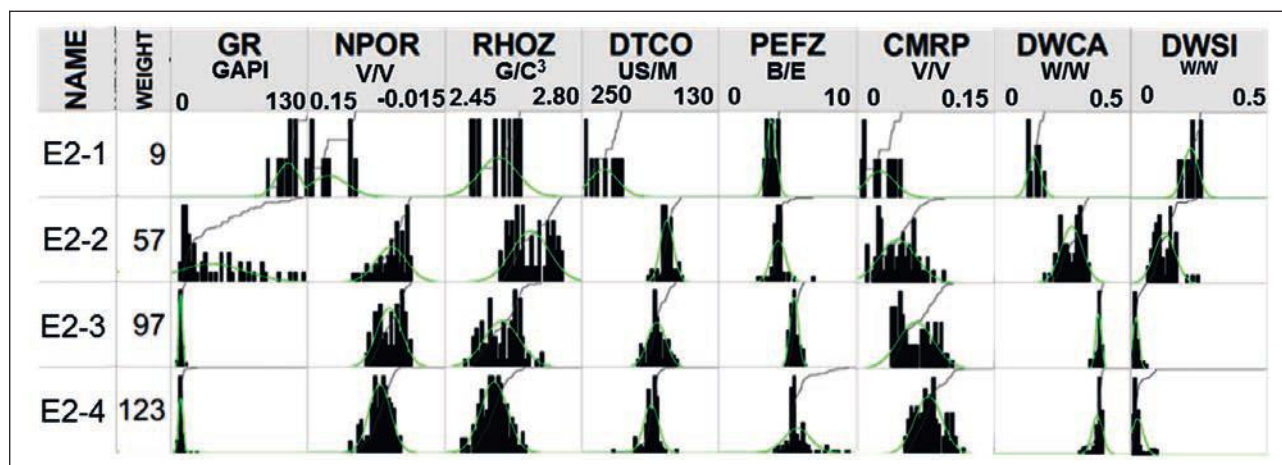


Figure 8 Synthesis of the electrofacies obtained for WELL-2, with the combination of generated clusters, and corresponding histograms for value variation from the wireline logs, with the best distinctions of values.

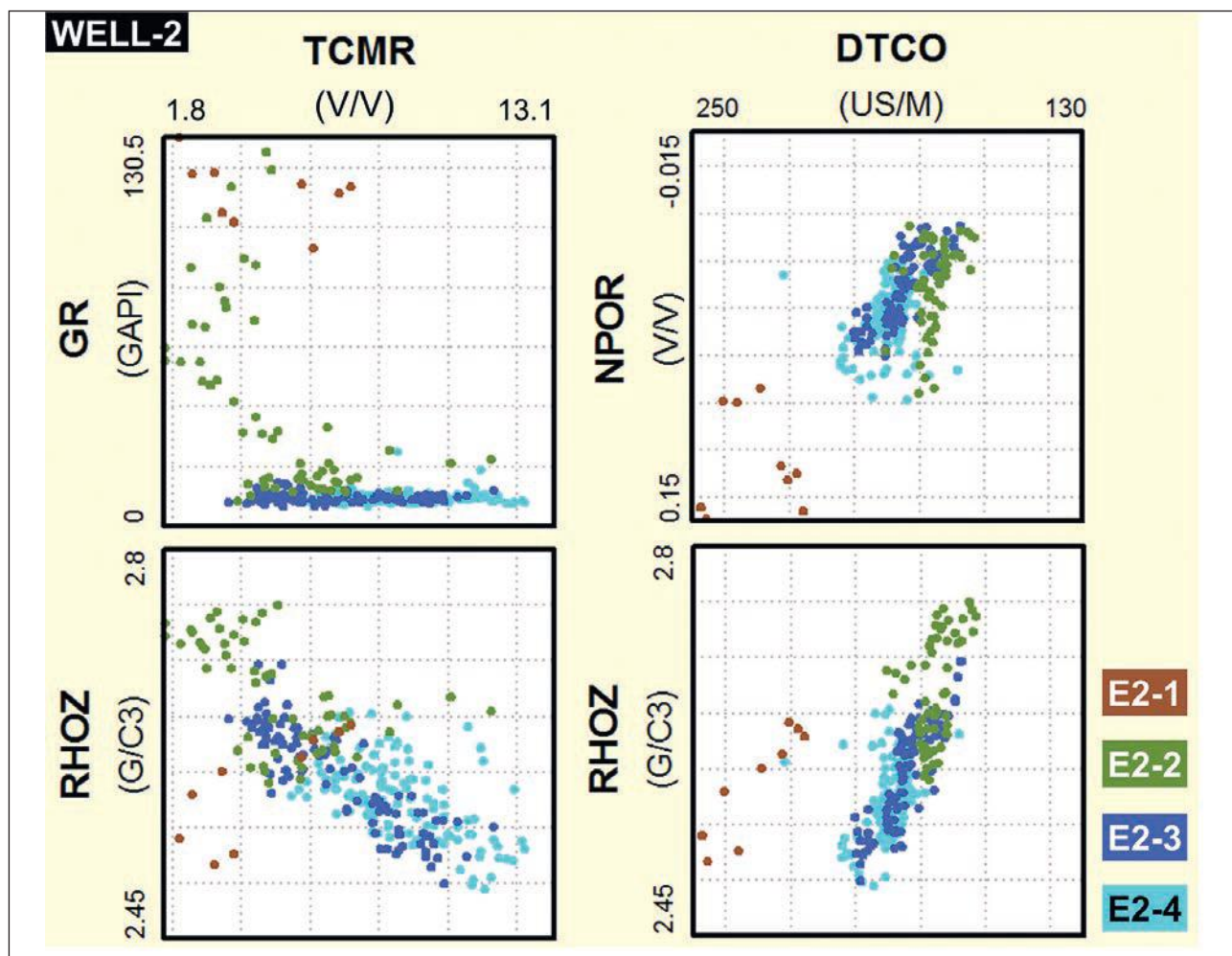


Figure 9 Electrofacies in wireline log crossplot for WELL-2.

The electrofacies E2-2 was created by combination of three clusters. It is characterized by gamma ray values from 10.6 to 67.7 API, with mean value of 39.1 API. Neutron results range from 0.079 and 0.026 v/v. The density generally ranges from 2.59 to 2.75 g/cm<sup>3</sup>. Acoustic transit times ranges from 180 to 170  $\mu$ s/m. The TCMR porosity ranges from 1.76 to 11.22%, with mean value of 5.08. The photoelectric effect (PE) ranges from 2.95 to 6.86 b/e, with mean value of 4.32 b/e. This electrofacies has calcium content ranging from 0.19 to 0.35 w/w, Si from 0.06 to 0.24 w/w, and very low aluminum content (DWA1), minimum value of 0.02 w/w. This electrofacies has strong correlation to the lithofacies coquina with carbonate mud (CQu), with probability of 82%.

The electrofacies E2-3 was formed by the combination of six clusters. The gamma ray ranges

from 7.12 to 11.3 API, with mean value of 9.5 API. Neutron log has values ranging from 0.077 to 0.0025 v/v. The density ranges from 2.52 to 2.66 g/cm<sup>3</sup>. Acoustic transit times range from 199 to 169  $\mu$ s/m. The TCMR porosity ranges from 3.36 to 11.30%, with mean value of 6.84%. The photoelectric effect (PE) ranges from 4.93 to 6.30 b/e, with mean value of 5.50 b/e. This electrofacies shows calcium content ranging from 0.35 to 0.4 w/w, and very low values of Si, Fe and Al. It corresponds to the lithofacies of poorly sorted massive coquina with variable degree of fragmentation (CQm), with 55% of probability.

The electrofacies E2-4 was generated by the combination of nine clusters. The gamma ray ranges from 6.4 to 13.0 API, with mean value of 9.6 API. Neutron porosity log has values ranging from 0.089 to 0.0039 v/v. The density log ranges from 2.520

	E2-1	E2-2	E2-3	E2-4
MOST	MD (100%)	CQu (82%)	CQm (55%)	CQf (60%)
		CQf (16%)	CQf (34%)	CQm (37%)
LEAST		CQm (2%)	CQu (11%)	CQu (3%)

Figure 10 Electrofacies by decreasing probability of lithofacies occurrence in WELL-2 (MD – mudstone; CQu - coquina with carbonate mud; CQf - coquina with moderate to high fragmented and/or oriented shell; CQm – poorly selected massive coquina with variable degree of fragmentation).

to 2.630 g/cm<sup>3</sup>. Acoustic transit times range from 204 to 180 μs/m. The TCMR porosity ranges from 5.45% to 13.06%, with mean value of 8.65%. The photoelectric effect (PE) ranges from 4.13 to 9.49 b/e, with mean value of 5.73 b/e. This electrofacies presents calcium content ranging from 0.32 to 0.4 w/w, and very low values of Si, Fe and Al. It is associated to the lithofacies of coquina with moderate to high degree of fragmentation and/or oriented shells (CQf), with 60% of probability.

## 5 Discussion

Electrofacies consists of a numerical representation of lithological stack patterns related to wireline logs (Rider, 2000). However, the result of this numerical representation often conflicts with the lithological description from cores, which are based on macroscopic characteristic and do not always correspond to the petrophysical variations of the analyzed rocks (Rosa, 2006).

The electrofacies modelling in WELL-1 turned out to correlate the definition of electrofacies and the lithofacies: coquina (CQ); hybrid rock (HB); mudstone (MD) and sandstone (SD) (Figure 11 Wireline logs, lithofacies description and electrofacies defined for WELL-1, characterized by a hybrid geological setting, Figure 11). The probabilistic correspondence between lithofacies and electrofacies varies from 61 to 69%. The two electrofacies with the most similar responses are the ones corresponding to coquina and hybrid rock, because both present carbonate grains, essentially bivalve shells, although the hybrid rocks also present stevensitic and si-

liclastic grains. The electrofacies E1-2, which are related to hybrid rocks, has slightly higher gamma ray and density values and slightly lower values of neutron porosity and acoustic transit time.

The electrofacies E1-3, related to mudstone, have a wide range of gamma ray values. This electrofacies includes distinct mudstones. The electrofacies E1-4, related to sandstones, has high gamma ray values, which is due to their constituents, feldspars, micas and volcanic rock fragments (Armeleni *et al.*, 2016).

In WELL-2, four electrofacies were defined related to: mudstone (MD); coquina with carbonate mud (CQu); coquina with moderate to high degree of shell fragmentation and/or oriented shells (CGf); poorly sorted massive coquina with variable degree of shell fragmentation (CQm) (Figure 12 – Wireline logs, lithofacies description and electrofacies defined for WELL-2, characterized by carbonate geological setting.). Although coquinas have the same composition, diagenetic processes and porosity are distinct, influencing the log responses. The electrofacies are mainly distinguished among each other in the porosity logs, such as neutron-density and RMN logs. The lithofacies with high degree of shell fragmentation and massive coquina generally shows higher porosity values, as well as massive coquinas and coquinas with mud. It is worth mentioning that the larger number of profiles used the more precise the electrofacies analysis. FMI log interpretation can be useful to characterize electrofacies, like realized by Muniz (2013).

Diagenetic processes such as dissolution, cementation and compaction influence the wireline logs response. Correa (2016) used electrofacies analysis to distinguish diagenetic products for a same facies association, studying bioclastic rudstone of Coqueiros Formation of Campos Basin. The diverse diagenetic processes that occurred in the same facies association may explain the large range of log values for a same electrofacies. Therefore, merged clusters formed the electrofacies because the main objective of this work was to distinguish depositional lithofacies.



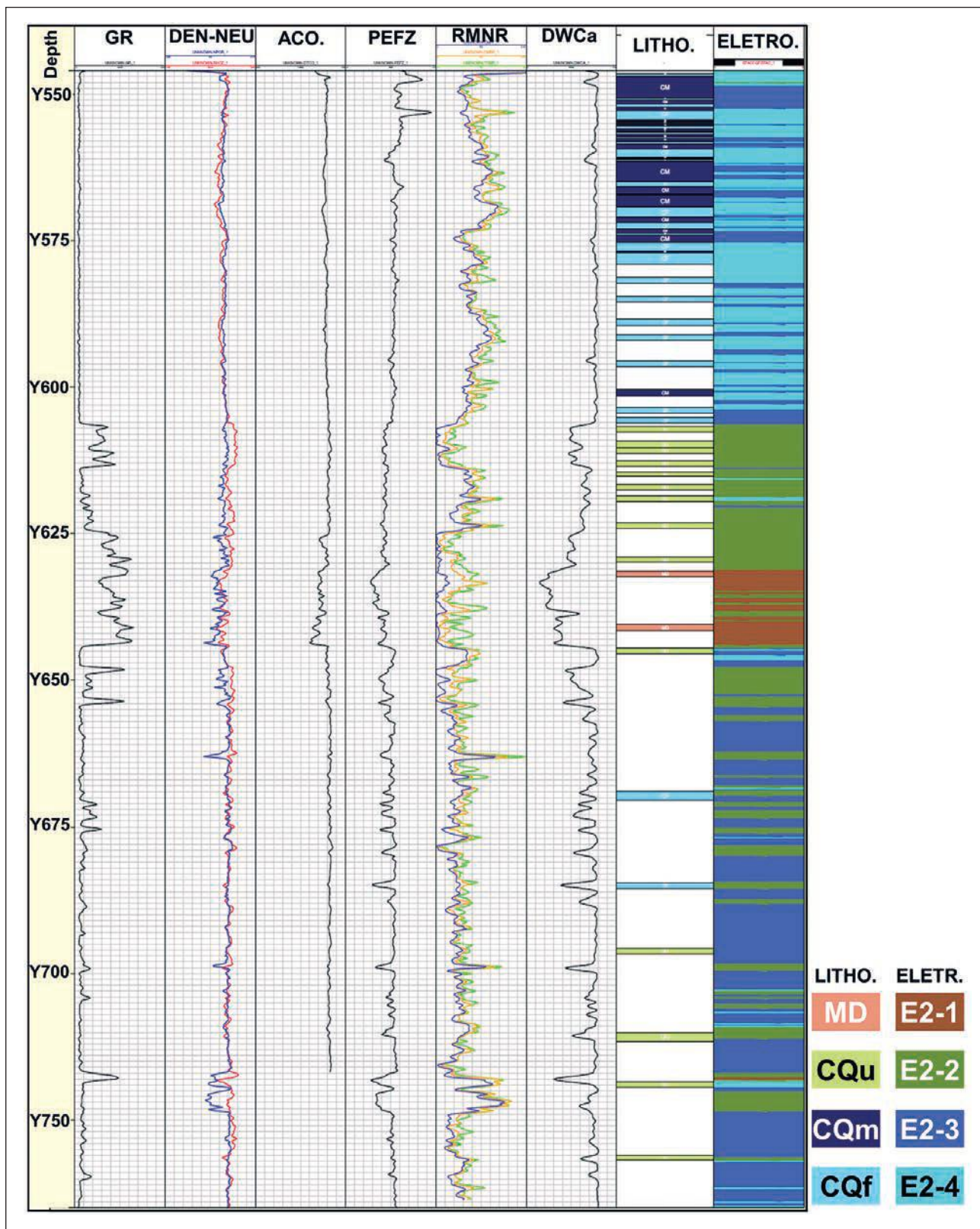


Figure 12 – Wireline logs, lithofacies description and electrofacies defined for WELL-2, characterized by carbonate geological setting.

Although there are some differences in the correlation between intervals of lithofacies and electrofacies, the electrofacies analysis proved to be efficient in distinguishing large stacking patterns with the main facies characteristics. This type of study can provide important information for sedimentological and reservoir interpretation. For example, in WELL-1, it is notorious the distinction between intervals with sandstones and mudstones intercalations and intervals with coquina and hybrid rock intercalations. In WELL-2, it is possible to make the distinction among three intervals: one with predominance of poorly sorted, massive coquina, another one with siliciclastic mudstone and mud rich coquina, and a third one with prevailing organized and highly fragmented shell coquina. Therefore, although it does not replace the direct and precise information obtained from the rock sampling, electrofacies modeling can be used in wells with little or no rock sampling, allowing geological and reservoir regional interpretations.

## 6 Conclusions

This work showed that the electrofacies analysis allows the distinction of lithofacies in bioclastic carbonate deposits, intercalated with hybrids and siliciclastic rocks. Although it is not always possible to distinguish lithofacies using wireline logs all the depositional facies. Several lithofacies could not be well distinguished in the electrofacies model because they do not have outstanding log responses. Nevertheless, it was still possible to do sedimentological and reservoir quality interpretations.

This study permits to extrapolate the lithofacies limit extrapolation by using wireline logs. There will always be an associated degree of uncertainty that must be taken into account. In the studied rocks the higher degrees of uncertainty in the correlation between the electro- and lithofacies were obtained with siliciclastic rocks. In WELL-1, it was also possible to distinguish carbonates and hybrid rocks. In WELL-2, the electrofacies model distinguishes carbonates from siliciclastic mudstone and also coquina with mud from other rocks, and individualizes coquina facies with respect to taphonomic criteria, by distinguishing coquina with moderate to high degree of shell fragmentation and/or oriented shells from

poorly sorted massive coquina with variable degree of shell fragmentation.

Electrofacies modeling can provide geological and reservoir regional interpretations and can be useful to complement geological interpretation in wells with little or no sampling. Nevertheless, the modeling will never be able to replace completely the rock sampling and studies.

## 7 Acknowledgements

The authors acknowledge the Brazilian National Petroleum Agency (ANP) for data liberation and Petrobras for access to samples and well logs, analysis support, and permission to publish this work. The authors also thank Rodolfo Araujo Victor for improvement suggestions.

## 8 References

- Agência Nacional do Petróleo, Gás Natural e Biocombustíveis - ANP. 2017a. 2ª Rodada de Partilha, Bacia de Santos, Sumário Executivo das Áreas em Oferta. Superintendência de Definição de Blocos, Superintendência de Exploração, Superintendência de Desenvolvimento e Produção. Rio de Janeiro, Brasil, 33p.
- Agência Nacional do Petróleo, Gás Natural e Biocombustíveis - ANP. 2017b. 3ª Rodada do Pré-sal, Bacia de Santos, Sumário Geológico e Áreas em Oferta. Superintendência de Definição de Blocos. Rio de Janeiro, Brasil, 12p.
- Al Ibrahim, M.A.; Sarg, J.F.; Hurley, N.; Cantrell, D.L. & Humphrey, J. 2017. Depositional environments and sequence stratigraphy of carbonate mudrocks using conventional geologic observations, multiscale electrofacies visualization, and geochemical analysis: The case of the Tuwaq Mountain and Hanifa Formations in a basinal setting, Saudi Arabia. *AAPG Bulletin*, 101: 683-714.
- Armelenti, G.; Goldberg, K.; Kuchle, J. & De Ros, L.F. 2016. Deposition, diagenesis and reservoir potential of non-carbonate sedimentary rocks from the rift section of Campos Basin, Brazil. *Petroleum Geoscience*, 22(3): 223-239.
- Bastos, G. & Luparelli, A. 2015. In: BACIA DE CAMPOS. SEMINÁRIO TÉCNICO-AMBIENTAL DA 13ª RODADA DE LICITAÇÕES-BLOCOS EXPLORATÓRIOS, ANP.
- Baumgarten, C.S. & Scuta, M.S. 1989. Geometria dos corpos carbonáticos do reservatório Macaé (Metade Superior), Campo de Pampa. *Boletim de Geociências da Petrobras*, 3(1/2): 49-57.
- Carlotto, M.A.; Da Silva, R.C.B.; & Yamato, A.A. 2017. Libra: A newborn giant in the Brazilian Presalt Province, in R. K. Merrill and C. A. Sternbach, eds., Giant fields of the decade 2000-2010: *AAPG Memoir*, 113: 165-176.
- Carminatti, M.; Wolff, B. & Gamboa, L.A.P. 2008. New exploratory frontiers in Brazil. In: 19TH WORLD

- PETROLEUM CONGRESS, Madrid, Spain, June 29–July 3, 2008.
- Chang, H.K.; Bender, A.A.; Kowsmann, R.O. & Mello, U.T. 1990. Origem e evolução termomecânica de bacias sedimentares. In: GABAGLIA, G.P.R. & MILANI, E.J. (ed.). Origem e Evolução de Bacias Sedimentares. Petrobras, Rio de Janeiro, p. 49-71.
- Conceição, J.C.J.; Zalán, P.V. & Wolff, S. 1988. Mecanismo, evolução e cronologia do rifte Sul-Atlântico. *Boletim de Geociências da Petrobras*, 2: 255-265.
- Dehler, N.M.; Magnavita, L.P.; Gomes, L.C.; Rigoti, C.A.; Oliveira, J.A.B.; Sant’anna, M.V. & Costa, F.G.D. 2016. The ‘Helmut’ geophysical anomaly: a regional left-lateral transtensional shear zone system connecting Santos and Campos basins, southeastern Brazil. *Marine Petroleum Geology*, 72: 412-422.
- Dias, J.L. 2005. Stratigraphy, sedimentology and volcanism of the Lower Cretaceous phase along eastern Brazilian continental margin. In: 14TH INTERNATIONAL CONGRESS OF THE IAS, 2005, Recife. Anais. Recife, p. 1-2.
- Dias, J.L.; Scarton, J.C.; Esteves, F.R.; Carminatti, M. & Guardado, L.R. 1990. Aspectos da evolução tectono-sedimentar e a ocorrência de hidrocarbonetos na Bacia de Campos. In: GABAGLIA, G.P.R., MILANI, E.J. (ed.). *Origem e Evolução de Bacias Sedimentares*. PETROBRAS, Rio de Janeiro, p. 333-360.
- Correa, C.R.A. 2016. *Controles estratigráficos e predição da paragenese diagenética dos carbonatos lacustres da Formação Coqueiros nos campos de Badejo, Trilha, Linguado e Pampo – Aptiano da Bacia de Campos (RJ)*. Dissertação de Mestrado. Instituto de Geociências da Universidade de São Paulo, 101p.
- Flexa, R.T.; Andrade, A. & Carrasquilla, A. 2004. Identificação de litotipos nos perfis de poço do Campo de Namorado (Bacia de Campos, Brasil) e do lago Maracaibo (Venezuela) aplicando estatística multivariada. *Revista Brasileira de Geociências*, 34(4): 571-578.
- Gomes, P.O.; Parry, J. & Martins, W. 2002. The Outer High of the Santos Basin, southern São Paulo Plateau, Brazil: Tectonic setting, relation to volcanic events and some comments on hydrocarbon potential: *AAPG Search and Discovery Article 90022*, p. 1–5.
- Grou, T.M.L. 2015. *Caracterização geológica da formação Carapebus da Bacia de Campos através da análise de eletrofácies*. Instituto de Geociências, Universidade Estadual de Campinas. Dissertação de Mestrado, 92p.
- Horschutz, P. & Scuta, M.S. 1992. Fácies-perfis e mapeamento de qualidade do reservatório de coquinas da Formação Lagoa Feia do Campo de Pampo. *Boletim de Geociências da Petrobras*, 6(1/2): 45-58.
- Johnson, H.; Levell, S. & Mohamad, A. 1987. Depositional controls of reservoir thickness and quality distribution in Upper Miocene shallow marine sandstones (Stage IVD) of the Erb West Field, Offshore Sabah, NW Borneo. *Bulletin of the Geological Society of Malaysia*, 21: 195-230.
- Mello, M.R. 2008. The Super Giant Great Lagoa Feia Petroleum System: The New Frontier of Exploration in the Pre-Salt Sequences of the Great Campos Basin, Brazilian. *AAPG Search and Discovery Article*. AAPG Annual Convention, San Antonio, Texas.
- Morais, J.M. 2013. *Petróleo em águas profundas: uma história tecnológica da Petrobras na exploração e produção offshore*. Brasília: IPEA, Petrobras, 424p.
- Muniz, M.C. 2013. *Tectono-Stratigraphic evolution of the Barremian-Aptian Continental Rift Carbonates in Southern Campos Basin, Brazil*. PhD Thesis – Royal Holloway University of London, Londres, 324p.
- Oliveira, V.C.B.; Assis, C.M.; Borghi, L.F. & Carvalho, I.S. 2019. Lacustrine coquinas and hybrid deposits from rift phase: Pre-Salt, lower Cretaceous, Campos Basin, Brazil. *Journal of South American Earth Sciences*, 95.
- Petersohn, E. & Abelha, M. 2013. Libra, Brazil pre-salt, geological assessment. National Agency of Petroleum Natural Gas and Biofuels (ANP). Available in: <[http://www.brasil-rounds.gov.br/arquivos/Seminarios\\_P1/Apresentacoes/partilha1\\_tecnico\\_ambiental\\_ingles.pdf](http://www.brasil-rounds.gov.br/arquivos/Seminarios_P1/Apresentacoes/partilha1_tecnico_ambiental_ingles.pdf)> Accessed in: March, 2015.
- Rangel, H.D. & Martins, C.C. 1998. Main exploratory compartments, Campos Basin. In: *Searching For Oil and Gas in the Land of Giants*. Search, Rio de Janeiro, Schlumberger, p. 32-40.
- Rezaeeparto, K.; Bonab, H.; Kadkhodaie, A.; Arian, M. & Hajkazemi, E. 2016. Investigation of Microfacies—Electrofacies and Determination of Rock Types on the Aptian Dariyan Formation NW Persian Gulf. *Open Journal of Geology*, 6: 58-78.
- Rider, M. 2000. *The Geological Interpretation of Well Logs*. Sutherland, Scotland. Second Edition, Rider-French Consulting Ltd., 280p.
- Rosa, H. 2006. *Estudo de caracterização de eletrofácies por meio de perfis geofísicos de poços e de amostras de testemunhos utilizando estatística multivariada*. PhD Thesis - Universidade Estadual de Campinas, Faculdade de Engenharia Mecânica e Instituto de Geociências, 230p.
- Schäfer, W. 1972. *Ecology and Paleogeology of Marine Environments*. Chicago: The University of Chicago Press, 568p.
- Schmitt, P.; Veronez, M.R.; Tognoli, F.M.W.; Todt, V.; Lopes, R.C. & Silva, C.A.U. 2013. Electrofacies modelling and lithological classification of coals and mud-bearing fine-grained siliciclastic rocks based on neural networks. *Earth Science Research*, 2(1): 193-208.
- Serra, O. & Abbot, H. 1982. The contribution of logging data to sedimentology and stratigraphy. SPE. 55th Annual Fall Technical Conference and Exhibition, Dallas, Texas, p. 117-131.
- Stinco, L.P. 2006. Core and log data integration: the key for determining electrofacies. In: SPWLA 47th ANNUAL LOGGING SYMPOSIUM, 7p.
- Tang, H.; Toomey, N. & Meddaugh, W.S. 2011. Using an artificial-neural-network method to predict carbonate well log facies successfully. *SPE Reservoir Evaluation & Engineering*, p. 35-44.
- Tang, H. & White, C.D. 2008. Multivariate statistical log log-facies classification on a shallow marine reservoir. *Journal of Petroleum Science & Engineering*, 61: 88–93.
- Ye, S.J. & Rabiller, P. 2000. A new tool for electro-facies analysis: Multi-Resolution Graph-Based Clustering. In: SPWLA 41<sup>st</sup> ANNUAL LOGGING SYMPOSIUM. Dallas, 14p.
- Ye, S.J. & Rabiller, P. 2005. Automated Electrofacies Ordering. *Petrophysics*, 46(6): 409-423.
- Winter, W.R.; Jahnert, R.J. & França, A.B. 2007. Bacia de Campos. *Boletim de Geociências da Petrobras*, 15: 511-529.